

Epigenomic translocation of H3K4me3 broad domains over oncogenes following hijacking of super-enhancers

Authors

Aneta Mikulasova¹, Daniel Kent^{1,2}, Marco Trevisan-Herraz¹, Nefeli Karataraki², Kent T.M. Fung², Cody Ashby³, Agata Cieslak⁴, Shmuel Yaccoby⁵, Frits van Rhee⁵, Maurizio Zangari⁵, Sharmilan Thanendarajan⁵, Carolina Schinke⁵, Gareth J. Morgan⁶, Vahid Asnafi⁴, Salvatore Spicuglia^{7,8}, Chris A. Brackley⁹, Anne E. Corcoran¹⁰, Sophie Hambleton^{2,11}, Brian A. Walker¹², Daniel Rico^{1*#}, Lisa J. Russell^{2*#}

Affiliations

¹Biosciences Institute, Newcastle University, Newcastle upon Tyne, UK

²Translational and Clinical Research Institute, Newcastle University, Newcastle upon Tyne, UK

³Department of Biomedical Informatics, University of Arkansas for Medical Sciences, Little Rock, AR USA

⁴Université de Paris (Descartes), Institut Necker-Enfants Malades (INEM), Institut national de la santé et de la recherche médicale (Inserm) U1151, and Laboratory of Onco-Hematology, Assistance Publique-Hôpitaux de Paris, Hôpital Necker Enfants-Malades, 75015 Paris, France

⁵Myeloma Center, University of Arkansas for Medical Sciences, Little Rock, AR USA

⁶NYU Langone Medical Center, Perlmutter Cancer Center, NYU Langone Health, New York City, NY, USA

⁷Aix-Marseille University, Inserm, Theories and Approaches of Genomic Complexity (TAGC), UMR1090, 13288 Marseille, France

⁸Equipe Labellisée Ligue Contre le Cancer

⁹SUPA, School of Physics and Astronomy, University of Edinburgh, Edinburgh, UK

¹⁰Lymphocyte Signalling and Development Programme, Babraham Institute, Cambridge, UK

¹¹Great North Children's Hospital, Newcastle upon Tyne Hospitals NHS Foundation Trust, UK

¹²Melvin and Bren Simon Comprehensive Cancer Center, Division of Hematology Oncology, Indiana University, Indianapolis, IN, USA

*Joint last authors

#Correspondence should be addressed to lisa.russell@newcastle.ac.uk or daniel.rico@newcastle.ac.uk.

Contents

Supplemental Results	3
Genome-wide H3K4me3-BD and super-enhancer co-occurrence	3
Supplemental Tables.....	4
Supplemental Table S1: Selected BLUEPRINT chromatin states and their characterization.	4
Supplemental Table S2: Overview of BLUEPRINT ChIP-seq samples from healthy donors and patients with B-cell haematological malignancies.	5
Supplemental Table S3: Characteristics of cell line derived from B-cell and T-cell haematological malignancies, data availability and sources.	6
Supplemental Table S4: List of 59,097 H3K4me3-BDs detected by genome-wide analysis.	7
Supplemental Table S5: Characteristics of seven patient derived xenograft multiple myeloma samples.	8
Supplemental Figures	9
Supplemental Figure S1: Immunoglobulin structure, genes and physiological genomic rearrangements.	9
Supplemental Figure S2: Overview of H3K4me3-BDs detected at genome-wide level.	10
Supplemental Figure S3: Genes annotated to H3K4me3-BD enrichment analysis for biological processes.	11
Supplemental Figure S4: Proximity of super-enhancers to H3K4me3-BDs or small promoters.	12
Supplemental Figure S5: Chromatin landscape of the human <i>IGH</i> locus (14q32) in five cell lines derived from B-cell haematological malignancies.	13
Supplemental Figure S6: Chromatin landscape of the <i>MYEOV</i> locus (11q13) in healthy human B cells and five cell lines derived from B-cell haematological malignancies.	14
Supplemental Figure S7: Chromatin landscape of the <i>MYC</i> (8q24) and <i>FGFR3/NSD2</i> (4p16) loci in healthy human B cells and multiple myeloma samples.	15
Supplemental Figure S8: Detailed chromatin landscape of <i>MYC</i> (8q24) and <i>FGFR3/NSD2</i> (4p16) loci in multiple myeloma samples.	16
Supplemental Figure S9: Genomic and epigenomic architecture of the <i>TRA/TRD</i> locus (14q11) in healthy and malignant human haematopoietic cells.	17
Supplemental Figure S10: Genomic and epigenomic architecture of the <i>BCL11B</i> locus (14q32) in healthy and malignant human haematopoietic cells.	18
Supplemental Figure S11: Genomic and epigenomic architecture of the <i>BCL11B</i> locus (14q32) in healthy and malignant human haematopoietic cells, detailed image.	19
Supplemental Figure S12: Genomic and epigenomic architecture of the <i>TAL1</i> locus (1p33) in healthy and malignant human haematopoietic cells.	20
Supplemental Figure S13: H3K4me3 and H3K27ac histone marks signal at <i>TAL1</i> locus in PEER cell line.	21

Supplemental Results

Genome-wide H3K4me3-BD and super-enhancer co-occurrence

A total of 59,097 (15,443 non-overlapping) H3K4me3-BDs were detected at genome-wide level using BLUEPRINT chromatin state data divided into the following haematopoietic cell types: haematopoietic stem cells (HSC), B cells, T cells, myeloid cells, MCL, CLL and MM. H3K4me3-BDs were classified into categories based on epigenomic specificity using their overlaps and active chromatin background (**Supplemental Fig. S2**). A total of 31, 302, 144 and 1186 H3K4me3-BDs were exclusively detected in HSC, B cells, T cells and myeloid cells, respectively. This indicates that the vast majority of H3K4me3-BDs remain stable during haematopoiesis.

We confirm that cell-type exclusive H3K4me3-BDs are associated with cell-identity genes (**Supplemental Fig. S3**). B-cell exclusive H3K4me3-BDs identified genes important in B-cell biology (for example immunoglobulin genes *IGH*, *IGK* and *IGL*, or *PAX5*, *MS4A1* and *CD22*). Similarly, T-cell identity genes were enriched within T-cell exclusive H3K4me3-BDs (for instance *CD2*, *GATA3*, *BCL11B* or *CD28*) and myeloid identity genes within myeloid exclusive H3K4me3-BDs (for instance *TAL1*, *CEBPA*, *IL18* or *IL1B*). In comparison, H3K4me3-BDs that were shared between B cells, T cells and myeloid cells were associated with genes involved in basic cell functions such as RNA processing or epigenetic modifications and so they are likely reflecting the house-keeping background rather than haematopoiesis.

Total of 64, 74 and 206 H3K4me3-BDs were identified in MCL, CLL and MM that were not present in B cells. The high number of H3K4me3-BDs observed in MM can be due to the exclusion of H3K4me3-BDs from B cells which may not be representative of myeloma cells derived from plasma cells. Analysis of H3K4me3-BDs in B-cell malignancies for example identified T-cell markers such as *CD2* or *CD247*, proto-oncogenes *YES1*, *ETV1*, or *MYCN* or other cancer-associated genes such as *SDC1*, *WNT5A*, *SIX4* or *BCAR1*. The complete list of H3K4me3-BDs and their epigenomic specificity and gene annotation is provided in **Supplemental Table S4**.

We observed a significantly higher co-occurrence of H3K4me3-BD and super-enhancers compared to H3K4me3-BD and promoters (**Supplemental Fig. S4**). This enrichment increased with H3K4me3-BD size and was highly significant within a 100 kb proximity across all tested healthy and malignant cell types. Co-occurrence with super-enhancers within 100 kb was stronger in H3K4me3-BDs exclusive for B cells and myeloid cells (**Supplemental Fig. S4D,F**). T-cell exclusive H3K4me3-BDs showed broader enrichment with super-enhancers present more frequently within 2 Mb proximity (**Supplemental Fig. S4E**). This may be a result of a small number of H3K4me3-BDs, but also it could be a specific mechanism present in T cells, highlighting the presence of longer-range genomic interactions.

Supplemental Tables**Supplemental Table S1: Selected BLUEPRINT chromatin states and their characterization.**

Original # ¹	Description	Histone marks high signal	Figure colour
State 9	Active canonical enhancer	H3K4me1 & H3K27ac	Orange
State 10	Active non-canonical H3K4me3+ enhancer	H3K4me1 & H3K4me3 & H3K27ac	Green
State 11	Active promoter	H3K4me3 & H3K27ac	Yellow
State 7	Repressed Polycomb regulatory region	H3K4me1 & H3K4me3 & H3K27me3	Light blue

¹Carrillo-de-Santa-Pau, Enrique, David Juan, Vera Pancaldi, Felipe Were, Ignacio Martin-Subero, Daniel Rico, Alfonso Valencia, and on behalf of The BLUEPRINT Consortium. 2017. “Automatic Identification of Informative Regions with Epigenomic Changes Associated to Hematopoiesis.” Nucleic Acids Research.

Supplemental Table S2: Overview of BLUEPRINT ChIP-seq samples from healthy donors and patients with B-cell haematological malignancies.

Healthy donors

Cell lineage	Cell type	Cell type detail	Markers	Tissue	n
-	HSC	Mobilized primary cells	CD34+	CB	3
Lymphoid	B cells	Naïve	CD19 ⁺ CD27 ⁻ IgD ⁺	VB or CB	6
		GC	CD19 ⁺ CD20 ^{hi} CD38 ^{med}	T	3
		Unswitched memory	CD19 ⁺ CD27 ⁺ IgM ⁺ IgD ⁺	VB	1
		Class-switched memory	CD19 ⁺ CD27 ⁺ IgA ⁺ IgG ⁺ or CD19 ⁺ CD27 ⁻ IgD ⁻	VB	3
	Plasma cells	-	CD20 ^{med} CD38 ^{high}	T	2
	T cells	Early cortical	TCR $\alpha\beta^-$ CD3 ⁻ CD4 ⁺ CD8 ⁺	Th	1 [#]
		Late cortical	TCR $\alpha\beta^+$ CD3 ^{+low} CD4 ⁺ CD8 ⁺	Th	1 [#]
		Helper, alphabeta	CD3 ⁺ CD4 ⁺ CD45RA ⁺	VB or CB	9
		Helper, alphabeta, central memory	CD3 ⁺ CD4 ⁺ CD45RA ⁻ CD62 ⁺	VB	1
		Cytotoxic, alphabeta	CD3 ⁺ CD8 ⁺ CD45RA ⁺	VB or CB	4
		Cytotoxic, alphabeta, effector memory	CD3 ⁺ CD8 ⁺ CD45RA ⁻ CD62L ⁻	VB	1
Myeloid	Neutrophils	Mature	CD66b ⁺ CD16 ⁺ or NA	VB or CB	1 3
		Band form	CD11b ⁺ CD16 ^{dim}	BM	3
		Segmented	CD11b ⁺ CD16 ⁺⁺	BM	2
	Eosinophils	Mature	CD66 ⁺ CD16 ⁻	VB	2
	Monocytes	Classical	CD14 ⁺ CD16 ⁻	VB or CB	5
	Macrophages	Resting (M0)	*	VB or CB	7
		Classically activated (M1)	*	VB or CB	7
		Alternatively activated (M2)	*	VB or CB	7
	Erythroblasts	-	CD36 ⁺ CD71 ⁺ CD235a ⁺	CB	2
	Megakaryocytes	-	CD34 ⁻ CD41 ⁺ CD42 ⁺	CB	2

Patients with B-cell haematological malignancies

Malignancy	Cell type	Markers	Tissue	n
CLL	Mature naïve (uCLL) or post GC B cells (mCLL)	-	VB	7
MCL	Mature naïve pre-GC B cells	-	VB	5
MM	Plasma cells	CD138 ⁺	BM	4

Abbreviations: HSC – Haematopoietic stem cells, GC – Germinal centre, CB – Cord blood, VB – Venous blood, T – Tonsils, Th – Thymus, BM – Bone marrow, CLL – Chronic lymphocytic leukemia, uCLL – CLL with unmutated Ig variable region, mCLL – CLL with somatically mutated immunoglobulin variable region, MCL – Mantle cell lymphoma, MM – Multiple myeloma, *for details see BLUEPRINT methods. Data source: Carrillo-de-Santa-Pau E, Juan D, Pancaldi V, Were F, Martin-Subero I, Rico D, et al. Automatic identification of informative regions with epigenomic changes associated to hematopoiesis. *Nucleic Acids Res.* 2017;45(16):9244-59. [#]ChIP-seq reads from multiple donors merged, for details see Cieslak A, Charbonnier G, Tesio M, Mathieu EL, Belhocine M, Touzart A, et al. Blueprint of human thymopoiesis reveals molecular mechanisms of stage-specific TCR enhancer activation. *J Exp Med.* 2020;217(9).

Supplemental Table S3: Characteristics of cell line derived from B-cell and T-cell haematological malignancies, data availability and sources.

Cell line	Malignancy	Cell type origin	Sex	Chromosomal translocation	Data source [#]		
					ChIP-seq	DNase I HS & RNA-seq	TS
JVM-2	MCL	Mature naïve pre-GC B cells	F	t(11;14)(q13;q32) <i>CCND1-IGH</i>	BLUEPRINT		
Z-138	MCL	Mature naïve pre-GC B cells	M	t(8;11;14)(q24;q13;q32) <i>MYC-CCND1-IGH</i>	BLUEPRINT	BLUEPRINT	
BL-2	BL	GC B cells	M	t(8;22)(q24;q11.2) <i>MYC-IGL</i>	BLUEPRINT		
DG-75	BL	GC B cells	M	t(8;14)(q24;q32) <i>MYC-IGH</i>	BLUEPRINT	BLUEPRINT	
KARPAS-422	DLBCL	GC B cells	F	t(14;18)(q32;q21) <i>IGH-BCL2</i>	BLUEPRINT	BLUEPRINT	
SU-DHL-5	DLBCL	GC B cells	F	none	BLUEPRINT	BLUEPRINT	
U266	MM	Plasma cells	M	t(11;14)(q13;q32) <i>CCND1-IGH</i>	BLUEPRINT	BLUEPRINT	MM
KMS11	MM	Plasma cells	F	t(4;8;14;16)(p16;q24;q32;q23) <i>NSD2-MYC-IGH-MAF</i>	MM		MM
MM1S	MM	Plasma cells	F	t(8;14;16)(q24;q32;q23) <i>MYC-IGH-MAF</i>	MM		MM
KOPT-K1	T-ALL	Immature T cells	M	t(11;14)(p13;q11) <i>LMO2-TRA/TRD</i>	GSE54379		
DND-41	T-ALL	Immature T cells	M	t(5;14)(q35;q32) <i>TLX3-BCL11B</i>	GSE54379		
Jurkat	T-ALL	Immature T cells	M	none*	GSE65687		
PEER	T-ALL	Immature T cells	F	none*	T-ALL		

Abbreviations: GC – Germinal center, DNase I HS – DNase I hypersensitivity, TS – Targeted DNA sequencing, MCL – Mantle cell lymphoma, BL – Burkitt lymphoma, DLBCL – Diffuse large B-cell lymphoma, MM – Multiple myeloma; T-ALL – T acute lymphoblastic leukemia. *Jurkat cell line has a 12 bp insertion upstream of the *TAL1* gene that generates a *de novo* super-enhancer. This insertion was introduced in PEER cell line using CRISPR-Cas9.

[#]Notes for data source:

BLUEPRINT: Carrillo-de-Santa-Pau E, Juan D, Pancaldi V, Were F, Martin-Subero I, Rico D, et al. Automatic identification of informative regions with epigenomic changes associated to hematopoiesis. Nucleic Acids Res. 2017;45(16):9244-59.

MM: ChIP-seq and DNA sequencing data of U266, KMS11 and MM1S provided by Brian Walker.

GSE54379: <https://www.ncbi.nlm.nih.gov/geo/query/acc.cgi?acc=GSE54379>.

GSE65687: <https://www.ncbi.nlm.nih.gov/geo/query/acc.cgi?acc=GSE65687>.

T-ALL: ChIP-seq of wild type and edited PEER cell line data provided by Salvatore Spicuglia.

Supplemental Table S4: List of 59,097 H3K4me3-BDs detected by genome-wide analysis. Abbreviations: HSC – Haematopoietic stem cells, B – B cells, T – T cells, M – Myeloid cells, MCL – Mantle cell lymphoma, CLL – Chronic lymphocytic leukemia, MM – Multiple myeloma. Overlapped H3K4me3-BDs can be recognized by the same labelling within “PART” column.

Supplemental Table S4 is attached as a separated file.

Supplemental Table S5: Characteristics of seven patient derived xenograft multiple myeloma samples.

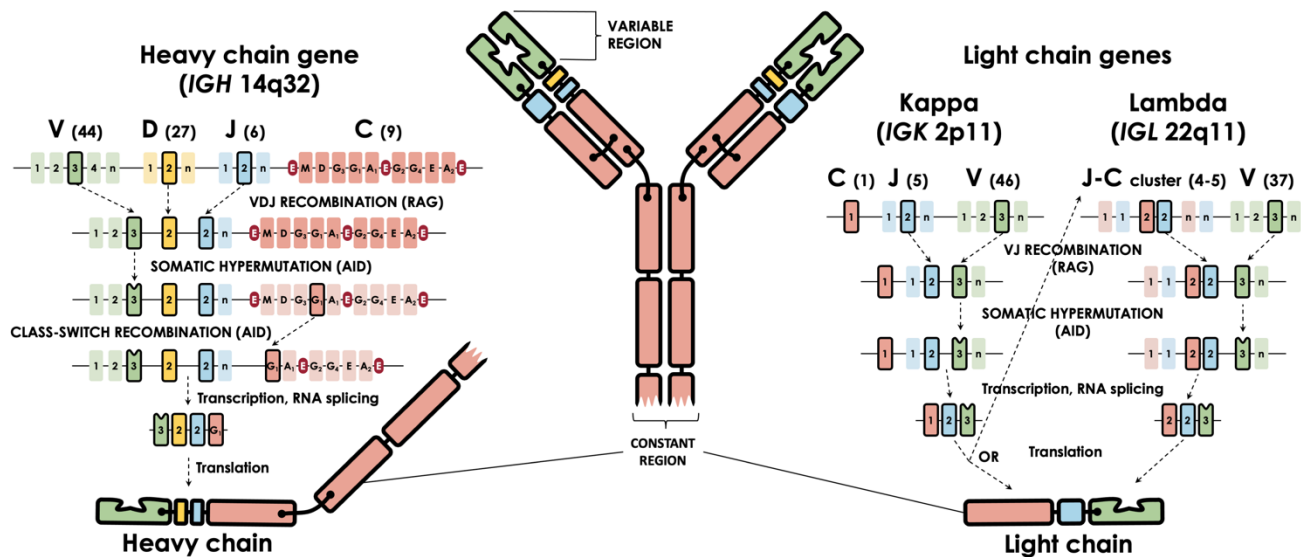
ID	Malignancy	Cell type origin	Sex	Chromosomal translocation	ChIP-seq	RNA-seq	WGS
P1	MM	Plasma cells	F	t(14;16)(q32;q23) <i>IGH-MAF</i>	yes	yes	yes
P2	MM	Plasma cells	F	t(14;16)(q32;q23) <i>IGH-MAF</i>	yes	-	yes
P3	MM	Plasma cells	F	t(4;14)(p16;q32) <i>NSD2-IGH</i>	yes	yes	yes
P4	MM	Plasma cells	M	Complex translocation involving <i>NSD2</i> and <i>IGH</i>	yes	yes	yes
P5	MM	Plasma cells	F	t(4;8)(q28;q24) <i>PCHD10-MYC</i>	yes	yes	yes
P6	MM	Plasma cells	M	none	yes	yes	yes
P7	MM	Plasma cells	M	none	yes	-	yes

Abbreviations: MM – Multiple myeloma, WGS – Whole genome sequencing.

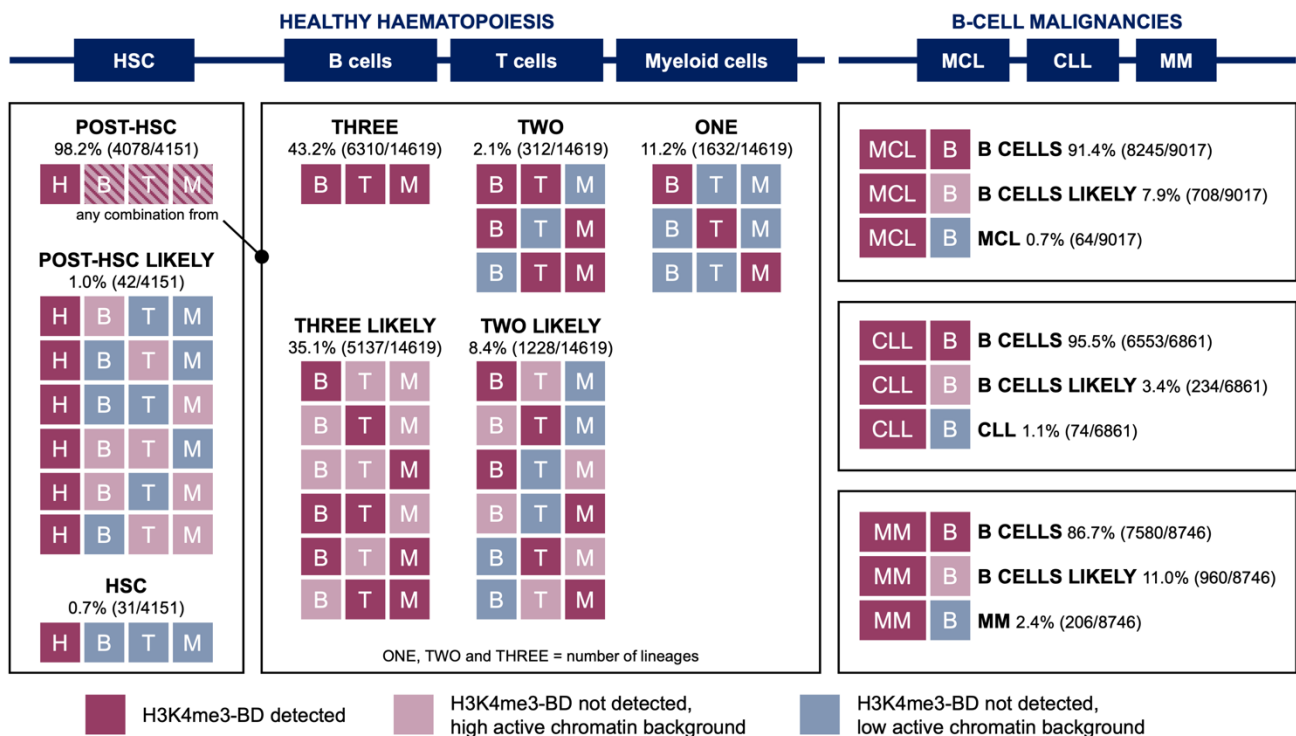
Supplemental Figures

Supplemental Figure S1: Immunoglobulin structure, genes and physiological genomic rearrangements.

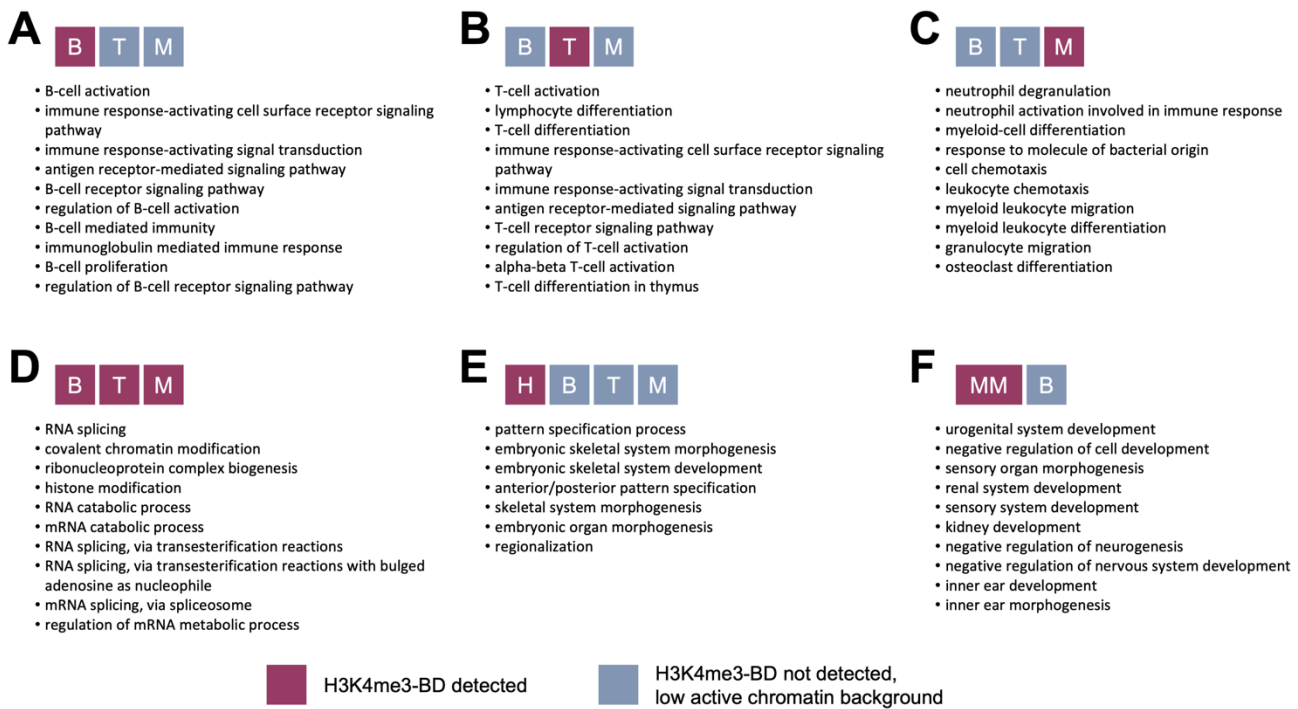
Abbreviations: C – Constant region, J – Joining region, D – Diversity region, V – Variable region, RAG – Recombination-activating gene, AID – Activation-induced cytidine deaminase.



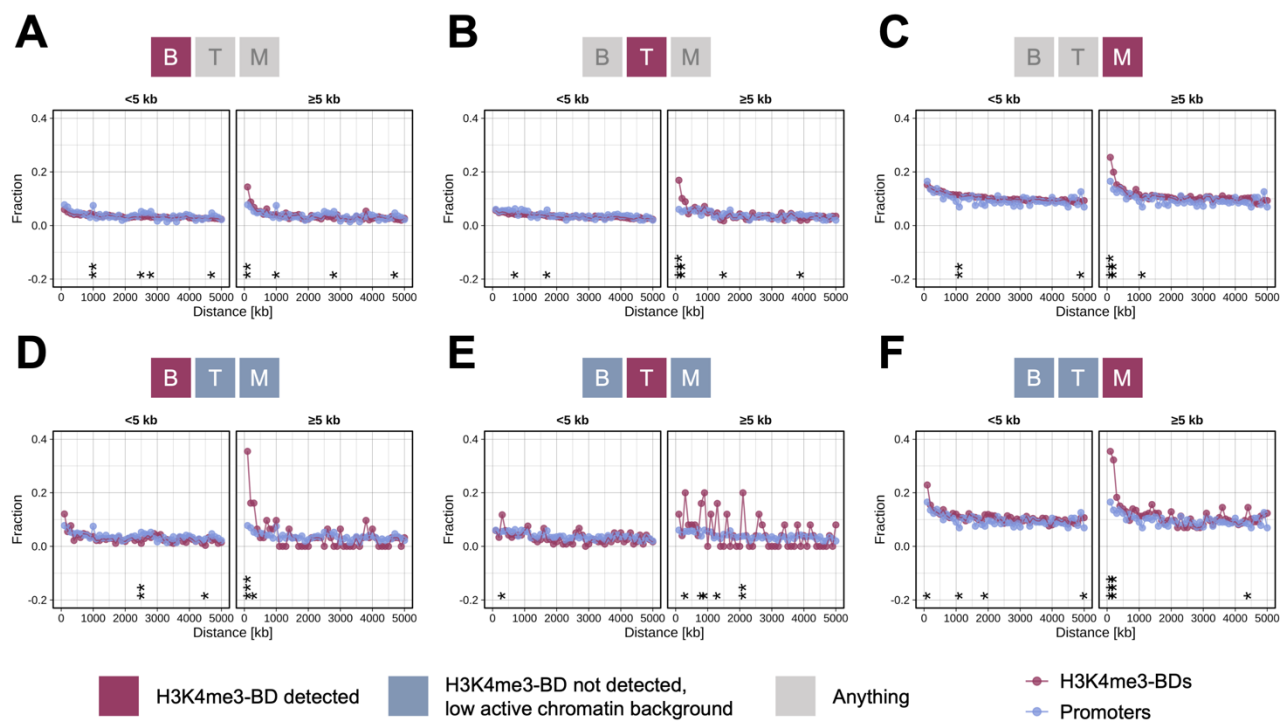
Supplemental Figure S2: Overview of H3K4me3-BDs detected at genome-wide level. Classification of H3K4me3-BD epigenomic specificity across healthy haematopoiesis and B-cell malignancies and proportions of each category within each group is shown. Abbreviations: H – Haematopoietic stem cells, B – B cells, T – T cells, M – Myeloid cells, MCL – Mantle cell lymphoma, CLL – Chronic lymphocytic leukemia, MM – Multiple myeloma.



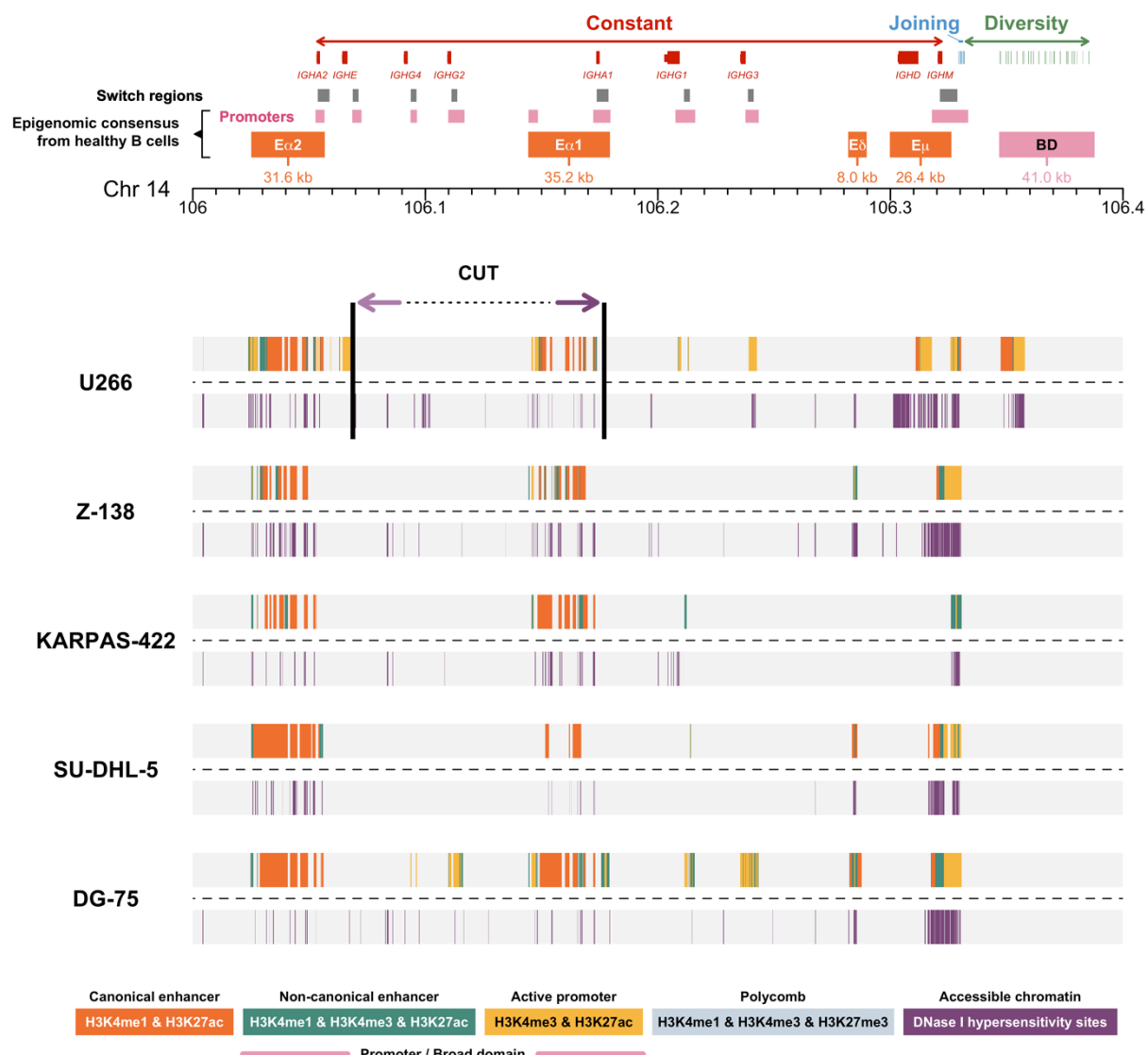
Supplemental Figure S3: Genes annotated to H3K4me3-BD enrichment analysis for biological processes. Selected categories of H3K4me3-BDs from **Supplemental Fig. S2** are shown as follow: H3K4me3-BDs exclusive for B cells (**A**), T cells (**B**) and myeloid cells (**C**), H3K4me3-BDs detected in all three lineages (B cells, T cells and myeloid cells) (**D**), H3K4me3-BDs exclusive for haematopoietic stem cells (**E**) and for multiple myeloma (**F**). First top 10 statistically significant biological processes are displayed. No significant enrichment was found in mantle cell lymphoma and chronic lymphocytic leukemia. Abbreviations: B – B cells, T – T cells, M – Myeloid cells, H – Haematopoietic stem cells, MM – Multiple myeloma.



Supplemental Figure S4: Proximity of super-enhancers to H3K4me3-BDs or small promoters. Each chart shows a fraction of H3K4me3-BDs (red dots) and promoters (blue dots) that have super-enhancer(s) within 100 kb distance windows in B cells (A, D), T cells (B, E), myeloid cells (C, F). Upper part (A–C) includes all H3K4me3-BDs detected in the given cell type and the lower part (D–F) shows only those H3K4me3-BDs recognized as cell type exclusive. Data for each chart are divided into two H3K4me3-BDs size intervals: from 2 kb to smaller than 5 kb (marked as <5 kb, on left) and 5 kb and bigger (marked ≥ 5 kb, on right). H3K4me3-BDs and promoter fractions were compared by Fisher's exact test. Statistically significant levels are as follows: ***P<0.001, **P<0.01 and *P<0.05. Abbreviations: B – B cells, T – T cells, M – Myeloid cells.



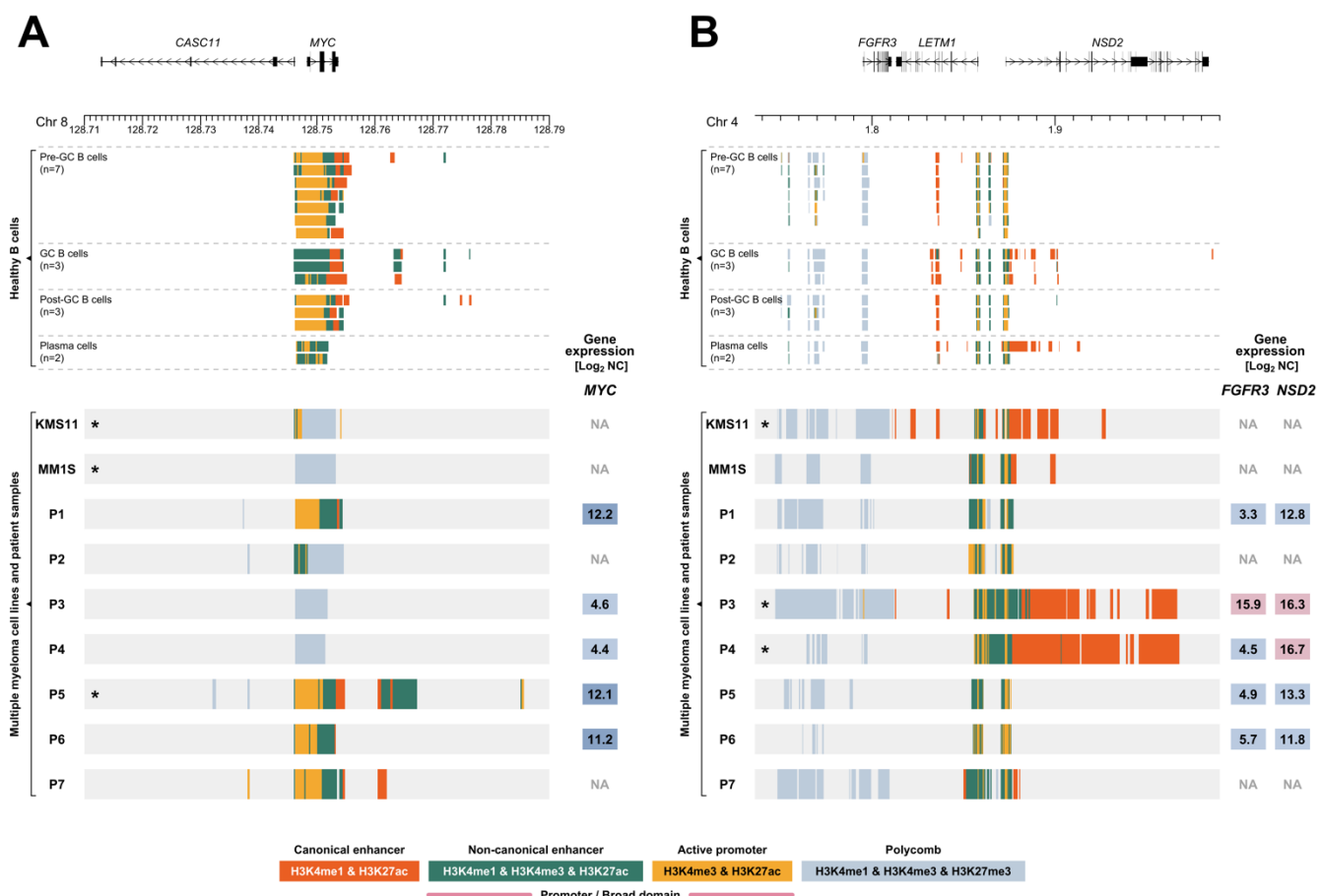
Supplemental Figure S5: Chromatin landscape of the human *IGH* locus (14q32) in five cell lines derived from B-cell haematological malignancies. Upper line of each cell line (Supplemental Table S3) represents the selected ChIP-seq chromatin states (Supplemental Table S1) and the lower line shows DNase I hypersensitivity sites for the non-variable region of the *IGH* locus. Vertical black lines in sample U266 mark breakpoint positions for the region, which includes the E α 1 super-enhancer that inserts \sim 12 kb upstream of *CCND1* (11q13). (Fig. 3). Abbreviations: BD – Broad domain.



Supplemental Figure S6: Chromatin landscape of the *MYEOV* locus (11q13) in healthy human B cells and five cell lines derived from B-cell haematological malignancies. Selected ChIP-seq chromatin states (Supplemental Table S1) of *MYEOV* gene in BLUEPRINT healthy B cells are shown in upper part. Upper line of each BLUEPRINT cell line in lower part represents the selected ChIP-seq chromatin states and the lower line shows DNase I hypersensitivity sites for the *MYEOV* locus. Numbers in coloured squares (red denotes high expression and blue low expression) show *MYEOV* expression detected using RNA-seq in Fragments Per Kilobase of transcript per Million mapped reads (FPKM). Abbreviations: GC – Germinal centre.

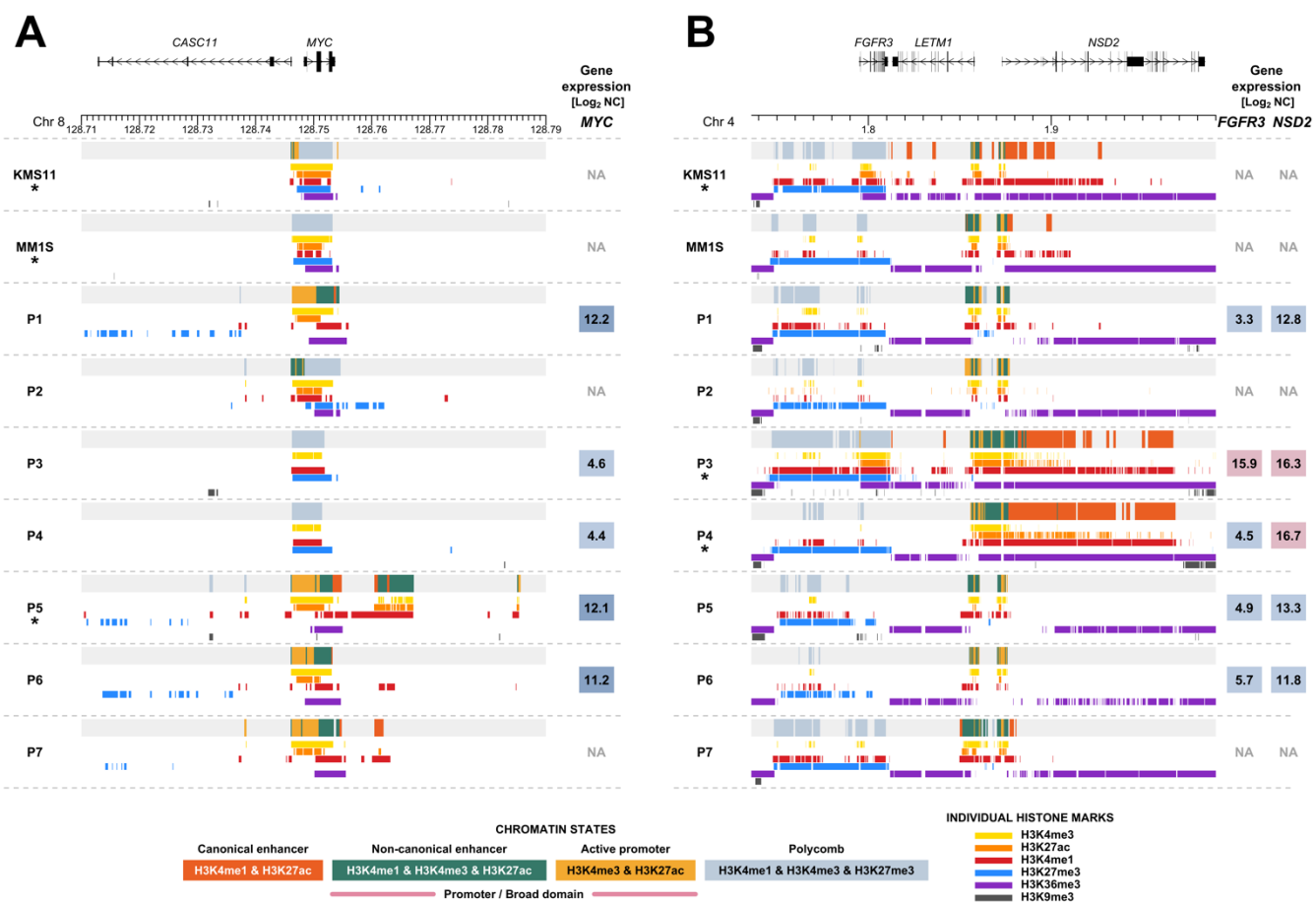


Supplemental Figure S7: Chromatin landscape of the *MYC* (8q24) and *FGFR3/NSD2* (4p16) loci in healthy human B cells and multiple myeloma samples. Upper panels show selected ChIP-seq chromatin states (Supplemental Table S1) of *MYC* (A) and *FGFR3/NSD2* (B) loci in BLUEPRINT healthy B cells. Each line of lower panel represents the ChIP-seq chromatin states for myeloma cell lines KMS11 and MM1S and seven multiple myeloma patients (P1-P7, patient derived xenograft material) for the *MYC* (A) and the *FGFR3/NSD2* (B) loci. Numbers in coloured squares (red denotes high expression and blue low expression; the two shades of blue for *MYC* expression denote different levels of low expression determined in our previous study¹) show gene expression detected by RNA-seq and displayed as Log₂ normalised counts (Log₂ NC). *sample contains chromosomal translocation involving the displayed region, described in detail in Supplemental Tables S3 and S5. Detailed picture of individual histone marks of the *MYC* and *FGFR3/NSD2* loci in multiple myeloma samples is given in Supplemental Fig. S8. Abbreviations: GC – Germinal centre.



¹Mikulasova, Aneta, Cody Ashby, Ruslana G. Tytarenko, Pingping Qu, Adam Rosenthal, Judith A. Dent, Katie R. Ryan, et al. 2019. "Microhomology-Mediated End Joining Drives Complex Rearrangements and over Expression of *MYC* and *PVT1* in Multiple Myeloma." *Haematologica*.

Supplemental Figure S8: Detailed chromatin landscape of *MYC* (8q24) and *FGFR3/NSD2* (4p16) loci in multiple myeloma samples. Each line represents ChIP-seq results for myeloma cell lines KMS11 and MM1S and seven multiple myeloma patients P1-P7, patient derived xenograft material) for the *MYC* (A) and the *FGFR3/NSD2* (B) loci. First line of each sample shows the selected ChIP-seq chromatin states (Supplemental Table S1) and other lines display peaks of individual histone marks. Numbers in coloured squares (red denotes high expression and blue low expression; the two shades of blue for *MYC* expression denote different levels of low expression determined in our previous study¹) show gene expression detected by RNA-seq and displayed as Log₂ normalised counts (Log₂ NC). *sample contains chromosomal translocation involving the displayed region, described in detail in Supplemental Tables S3 and S5.



¹Mikulasova Aneta, Cody Ashby, Ruslana G. Tytarenko, Pingping Qu, Adam Rosenthal, Judith A. Dent, Katie R. Ryan, et al. 2019. "Microhomology-Mediated End Joining Drives Complex Rearrangements and over Expression of *MYC* and *PVT1* in Multiple Myeloma." *Haematologica*.

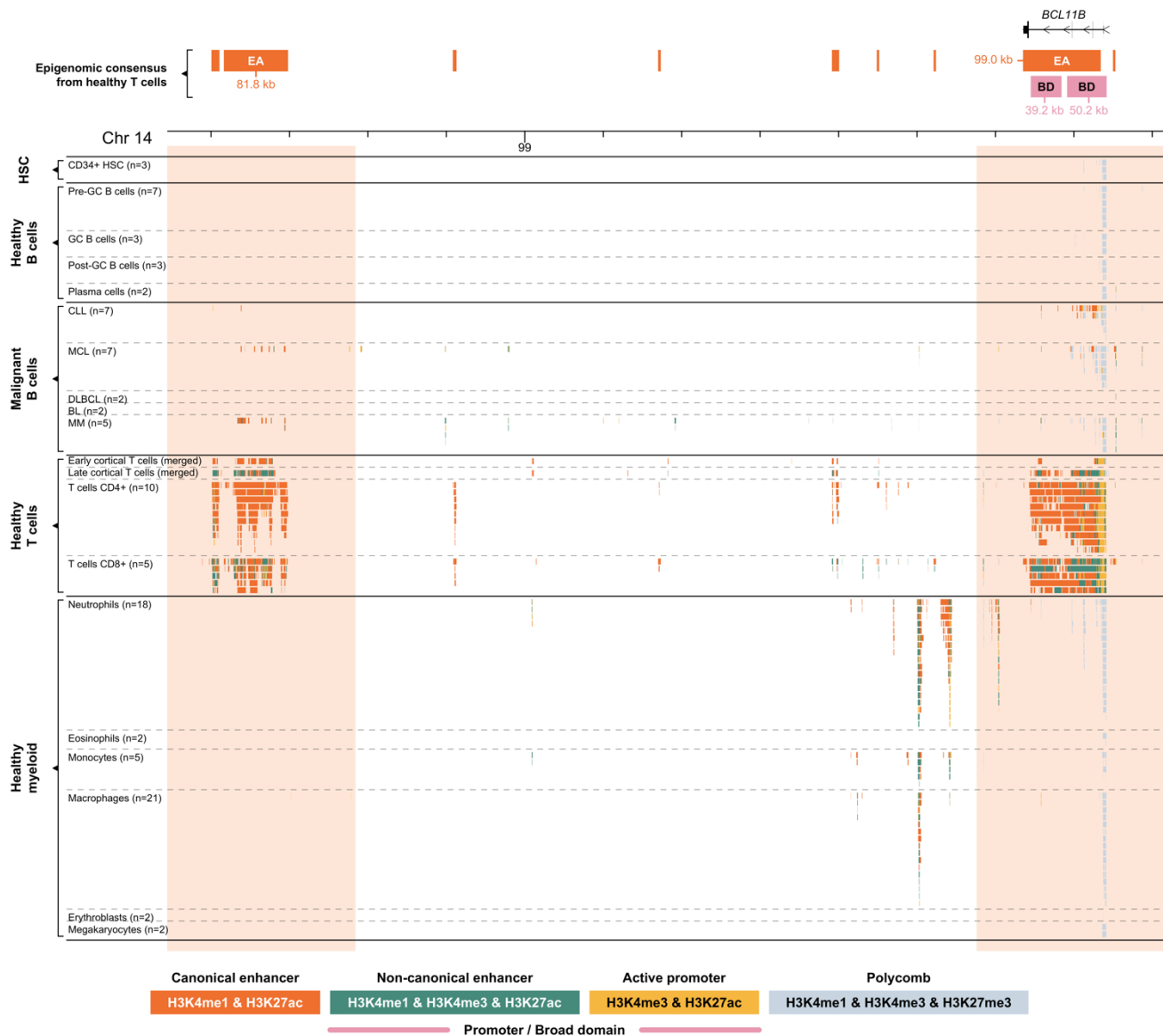
Footnote:

The H3K4me3-BD over *MYC* was missed by the chromatin state model in cell lines KMS11 and MM1S. This pattern was also observed in patient P2 despite no evidence of a translocation event. This observation remains unexplained. Additionally, a different epigenomic pattern over *MYC* was found in patient P5 with t(4;8). This difference can be explained by the presence of copy-number neutral loss of heterozygosity at 8q involving *MYC* locus and involvement of both alleles in *MYC* translocation, confirmed by whole genome sequencing alignments (data not shown). KMS11, P3 and P4 samples with a translocation involving the *FGFR3/NSD2* locus show a similar epigenomic pattern over the two genes, excluding *FGFR3* for patient P4. This difference is explained by the presence of a complex translocation in P4 sample involving monoallelic deletion of *FGFR3* gene, confirmed by in-depth analysis of whole genome sequencing (data not shown). KMS11 expresses high levels of *FGFR3* and *NSD2* (559 and 49 FKPM, respectively).

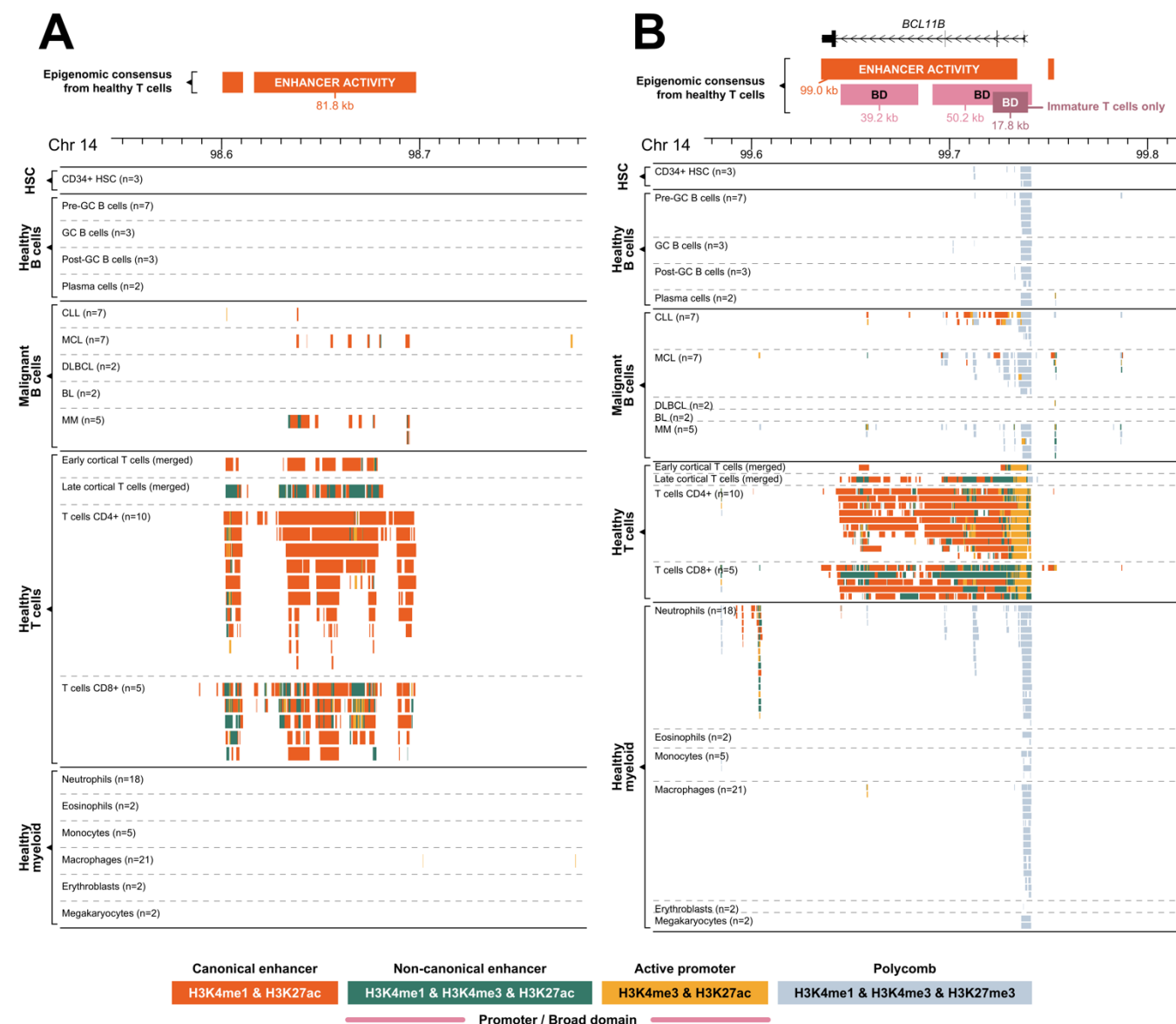
Supplemental Figure S9: Genomic and epigenomic architecture of the *TRA/TRD* locus (14q11) in healthy and malignant human haematopoietic cells. Each panel represents collapsed cell-type specific signals of ChIP-seq chromatin states included in this study (Supplemental Table S1). Abbreviations: HSC – Haematopoietic stem cells, GC – Germinal centre, CLL – Chronic lymphocytic leukemia, MCL – Mantle cell lymphoma, DLBCL – Diffuse large B-cell lymphoma, BL – Burkitt lymphoma, MM – Multiple myeloma.



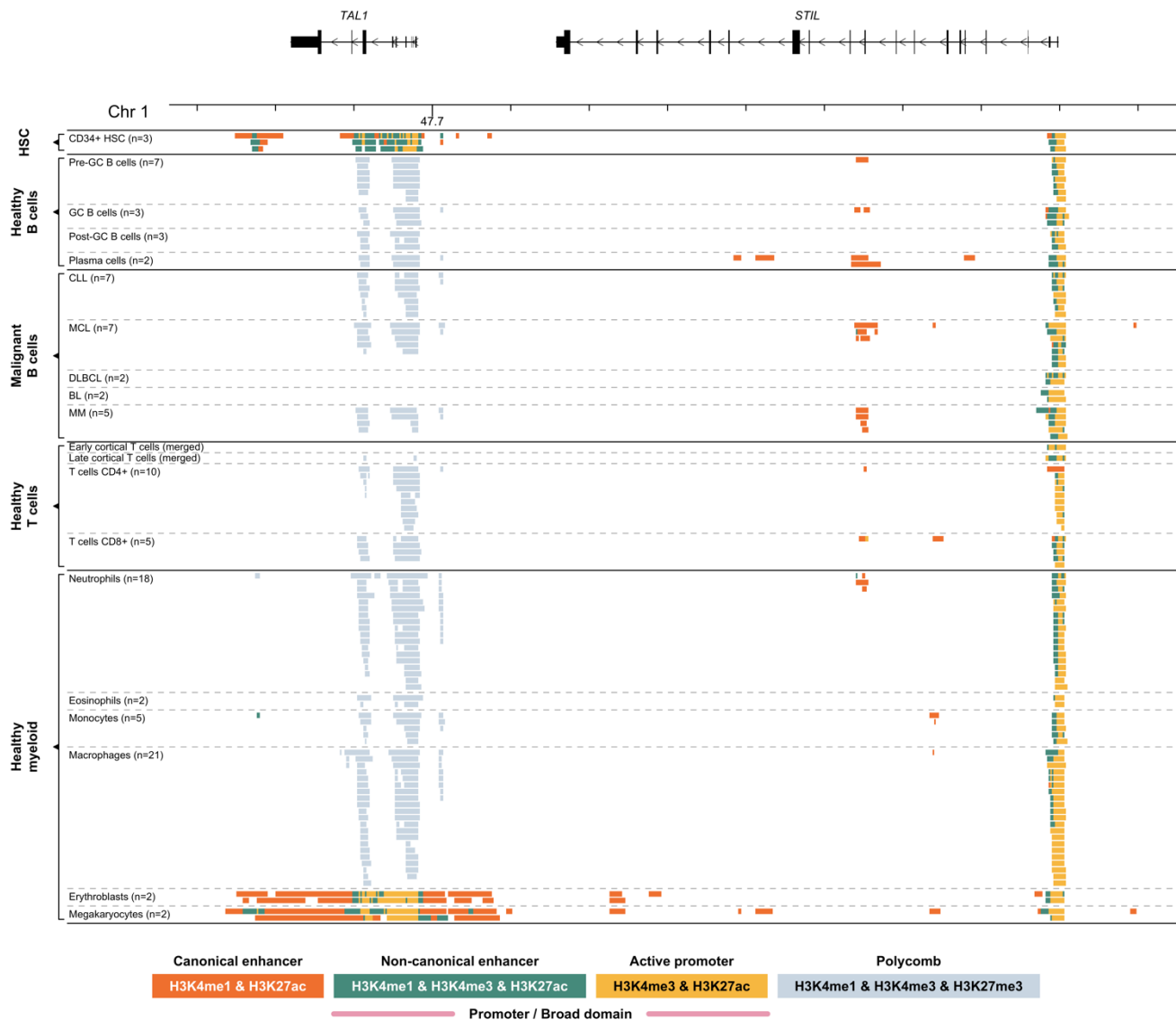
Supplemental Figure S10: Genomic and epigenomic architecture of the *BCL11B* locus (14q32) in healthy and malignant human haematopoietic cells. Each panel represents collapsed cell-type specific signals of ChIP-seq chromatin states included in this study (Supplemental Table S1). Areas with orange background mark regions showed in detail at Supplemental Fig. S11. Abbreviations: HSC – Haematopoietic stem cells, GC – Germinal centre, CLL – Chronic lymphocytic leukemia, MCL – Mantle cell lymphoma, DLBCL – Diffuse large B-cell lymphoma, BL – Burkitt lymphoma, MM – Multiple myeloma.



Supplemental Figure S11: Genomic and epigenomic architecture of the *BCL11B* locus (14q32) in healthy and malignant human haematopoietic cells, detailed image. Two regions marked by orange background in **Supplemental Fig. S10** are shown: intergenic super-enhancer activity in ~1 Mb proximity to *BCL11B* gene (**A**), and *BCL11B* gene (**B**). Each panel represents collapsed cell-type specific signals of ChIP-seq chromatin states included in this study (**Supplemental Table S1**). Abbreviations: HSC – Haematopoietic stem cells, GC – Germinal centre, CLL – Chronic lymphocytic leukemia, MCL – Mantle cell lymphoma, DLBCL – Diffuse large B-cell lymphoma, BL – Burkitt lymphoma, MM – Multiple myeloma.



Supplemental Figure S12: Genomic and epigenomic architecture of the *TAL1* locus (1p33) in healthy and malignant human haematopoietic cells. Each panel represents collapsed cell-type specific signals of ChIP-seq chromatin states included in this study (Supplemental Table S1). Abbreviations: HSC – Haematopoietic stem cells, GC – Germinal centre, CLL – Chronic lymphocytic leukemia, MCL – Mantle cell lymphoma, DLBCL – Diffuse large B-cell lymphoma, BL – Burkitt lymphoma, MM – Multiple myeloma.



Supplemental Figure S13: H3K4me3 and H3K27ac histone marks signal at *TAL1* locus in PEER cell line. 12bp DNA insertion known from Jurkat cell line upstream of *TAL1* gene was introduced in PEER cell line using CRISPR-Cas9. Normalized read count is shown for wild-type PEER in black and for edited PEER in red.

